

*Nucl. Phys., 1967, v. 96A,  
N 2, p. 258-272*

S-70

ОБЪЕДИНЕННЫЙ  
ИНСТИТУТ  
ЯДЕРНЫХ  
ИССЛЕДОВАНИЙ

Дубна

E-4-2934



ЛАБОРАТОРИЯ ТЕОРЕТИЧЕСКОЙ ФИЗИКИ

A. Sobiczewski

EQUILIBRIUM DEFORMATIONS OF HEAVY  
NUCLEI CALCULATED WITH PROJECTED  
WAVE FUNCTIONS

1966

4537/3 up.

A. Sobiczewski<sup>x/</sup>

EQUILIBRIUM DEFORMATIONS OF HEAVY  
NUCLEI CALCULATED WITH PROJECTED  
WAVE FUNCTIONS

Submitted to Nucl. Phys.

---

<sup>x/</sup> On leave of absence from and present address: Institute for  
Nuclear Research, Warsaw, Hoza 69, Poland.



## 1. Introduction

In the previous paper<sup>/1/</sup> the projected wave functions (PBCS) corresponding to a definite number of particles have been used to calculate the ground state equilibrium deformations, electric quadrupole moments and deformation energies for even nuclei in the rare earth region. It has been found that the use of the PBCS wave functions, instead of the BCS ones<sup>/2/</sup>, results in the increase of the equilibrium deformation (and the quadrupole moment): slight in the middle of the region and stronger at its boundaries. It also results in an earlier appearance (already for the  $^{142}\text{Ce}$  nucleus) of the deformation. As the quadrupole moments calculated with the help of the BCS wave functions<sup>/2/</sup> are larger than the experimental ones in the first half of the region (up to the Dy isotopes) and smaller in the second half (for Yb and heavier isotopes) the use of the PBCS wave functions increases the discrepancy in the first part of the region and decreases it in the second part. All this concerns the results, when the explicit Coulomb term, corresponding to a charged nucleus with a uniform or a trapezoidal charge distribution, is included into the energy. However, as it has been pointed out in a few papers (e.g. refs.<sup>/4,5/</sup>), some part of the Coulomb energy is probably taken into account by the use of the single-particle level scheme for protons different from that for neutrons. It was the reason that the calculation of ref.<sup>/1/</sup> was performed in two variants: one including the explicit Coulomb term and the other not. The values of the quadrupole moments obtained in the second variant (when the Coulomb term is dropped) show better agreement with experiment, especially at the beginning of the region. Also the point of appearance of the deformation (the neutron number  $N = 86-88$ ) agrees better with the point ( $N = 88-90$ ) deduced from such effects as appearance of rotational bands, sharp increase in the Coulomb excitation cross sections and an anomaly in the binding energy values of the last pair of neutrons<sup>/6/</sup>. At last the deformation energy, calculated in this variant, agrees better with the semi-empirical estimate<sup>/7/</sup> than in the variant including the explicit Coulomb term.

The aim of the present paper is to extend the calculations of ref.<sup>[1]</sup> to the heavy element region, and compare the results with the ones obtained with the BCS wave functions<sup>[3]</sup>. It is also aimed to check explicitly, at least for a few isotopes, what is the effect on the equilibrium deformation, quadrupole moment and deformation energy, of using the single-particle energy scheme for protons other than for neutrons.

## 2. Description of the Calculation

### 2.1. Method of the Calculation

We start with the Hamiltonian including the pairing forces in the approximation of constant matrix element, i.e.

$$H = H_{sp} + H_{pair} = \sum_{\nu} \epsilon_{\nu} (c_{\nu+}^{\dagger} c_{\nu+} + c_{\nu-}^{\dagger} c_{\nu-}) - G \sum_{\nu, \omega} c_{\nu+}^{\dagger} c_{\nu-}^{\dagger} c_{\omega-} c_{\omega+} \quad (1)$$

for neutrons and protons separately.

Here  $\epsilon_{\nu}$  is the energy of a twofold degenerate single-particle Nilsson state  $|\nu\rangle$ ,  $c_{\nu}^{\dagger}$  is the corresponding creation operator and  $G$  is the pairing force strength. The projected ground state wave function (PBCS - in the nomenclature of ref.<sup>[8]</sup>) is constructed by projecting fixed-particle terms from the BCS<sup>[9]</sup> wave function. When normalized it has the form<sup>[10,8]</sup>

$$|PBCS\rangle = \beta_1^{\dagger} \dots \beta_{\ell}^{\dagger} N \sum_{\nu_1 < \nu_2 < \dots < \nu_k} \gamma_{\nu_1} \dots \gamma_{\nu_k} \beta_{\nu_1}^{\dagger} \dots \beta_{\nu_k}^{\dagger} |vac\rangle, \quad (2)$$

where  $\gamma_{\nu} = v_{\nu} / u_{\nu}$ ,  $\beta_{\nu} = c_{\nu+}^{\dagger} c_{\nu-}^{\dagger}$  and the normalization factor

$$N = \left( \sum_{\nu_1 < \nu_2 < \dots < \nu_k} \gamma_{\nu_1}^2 \dots \gamma_{\nu_k}^2 \right)^{-1/2}.$$

The indices  $i = 1, \dots, \ell$  enumerate the levels with  $v_i = 1$  while the indices  $\nu_i$  ( $i = \ell, \dots, k$ ) correspond to the levels with  $0 < v_{\nu_i} < 1$ , i.e. to the levels between which the scattering of particles, due to the pairing interaction, takes place. We have the equality  $2(1 + k) = n$ , where  $n$  is the number of particles (neutrons or protons). The summation extends over all the combinations of  $k$  states (ordered with respect to the energy) chosen from the states, for which  $0 < v < 1$ . The symbol  $|vac\rangle$  denotes the vacuum for the particles described by the creation operators  $c_i^{\dagger}$  and  $c_{\nu_i}^{\dagger}$ .

The values of the variational parameters  $v_\nu$  ( $u_\nu^2 = 1 - v_\nu^2$ ) in the wave function (2) are established by minimization of the mean value of the Hamiltonian (1) in the BCS ground state<sup>9/</sup>, under the condition that the mean value of the number of particles in this state is given. The result is

$$2v_\nu^2 = 1 - (\epsilon_\nu - \lambda)/E_\nu \quad (3)$$

with  $E_\nu = \sqrt{(\epsilon_\nu - \lambda)^2 + \Delta^2}$ .

The chemical potential  $\lambda$  and the energy gap  $2\Delta$  are obtained from the equations

$$\begin{aligned} 2/C &= \sum_\nu 1/E_\nu \\ n &= \sum_\nu 2v_\nu^2 \end{aligned} \quad (4)$$

where  $n$  is the number of particles (neutrons or protons) in the nucleus.

The energy in the state (2) has the form<sup>10,8/</sup>

$$\begin{aligned} \mathcal{E} &= \sum_{i=1}^{\ell} 2\epsilon_i + N^2 \left\{ \sum_{\nu_1 < \nu_2 < \dots < \nu_k} 2(\epsilon_{\nu_1} + \dots + \epsilon_{\nu_k}) \gamma_{\nu_1}^2 \dots \gamma_{\nu_k}^2 - \right. \\ &\quad \left. - C \sum_{\sigma_1, \sigma_2} \gamma_{\sigma_1} \gamma_{\sigma_2} \sum_{\nu_2 < \nu_3 < \dots < \nu_k} \gamma_{\nu_2}^2 \dots \gamma_{\nu_k}^2 \right\} \end{aligned} \quad (5)$$

and the electric quadrupole moment

$$Q_0 = \sum_{i=1}^{\ell} 2q_{ii} + N^2 \sum_{\nu_1 < \nu_2 < \dots < \nu_k} 2(q_{\nu_1 \nu_1} + \dots + q_{\nu_k \nu_k}) \gamma_{\nu_1}^2 \dots \gamma_{\nu_k}^2 \quad (6)$$

where  $q_{\nu\nu}$  is the matrix element of the quadrupole moment operator in the single-particle state  $|\nu\rangle$ .

For the nuclei we consider here, neutrons and protons occupy states in the different shells and they are not correlated by the pairing forces. For this reason we solve eqs. (4) for neutrons and protons separately, with different single-particle level schemes and different pairing force strengths assumed. The total ground state energy of a nucleus is the sum of the energies of the neutron and proton systems. With Coulomb term  $\mathcal{E}_C$  included, it is of the form

$$\xi = \xi_n + \xi_p + \xi_c, \quad (7)$$

where  $\xi_n$  and  $\xi_p$  are given by eq. (5) and correspond to neutrons and protons, respectively.

The electric quadrupole moment of the nucleus is given by eq. (6) with the summation extended only over the proton states, i.e.

$$Q_0 = Q_p. \quad (8)$$

The Coulomb term in eq. (7) is assumed to be the electrostatic energy of a charged ellipsoid with a distribution of charge for which the surfaces of constant density form a family of similar concentric ellipsoids. In the case of axial symmetry the dependence of this energy on the deformation  $\bar{\epsilon}$  of the ellipsoid is given, up to the third order in  $\bar{\epsilon}$ , by<sup>11/</sup>

$$\xi_c(\bar{\epsilon}) = \left( 1 - \frac{4}{45} \bar{\epsilon}^2 - \frac{92}{2835} \bar{\epsilon}^3 \right) \xi_c(0). \quad (9)$$

Here  $\xi(0)$  is the electrostatic energy of the sphere from which the ellipsoid is obtained by a volume-preserving deformation. The definition of the parameter  $\bar{\epsilon}$  of the deformation of the equi-density ellipsoids is the same as the definition of the parameter  $\epsilon$  of the deformation of the equi-potential ellipsoids given in the Nilsson paper<sup>12/</sup>.

For each value of the parameter  $\epsilon$  the deformation  $\bar{\epsilon}$  is calculated from the formula

$$Q_0(\epsilon) = \bar{\epsilon} \left( 1 + \frac{1}{2} \bar{\epsilon} \right) \frac{4}{3} \int \rho(r') r'^2 d\vec{r}', \quad (10)$$

where  $\rho(r')$  is the charge density and  $Q_0(\epsilon)$  is the quadrupole moment obtained with the help of eq. (6).

## 2.2. Numerical Calculations

The values of the parameters of the single-particle Nilsson levels, used in the calculations, are given in table 1 with  $\hbar\omega = 41 A^{-1/3}$  MeV. A numerical value  $\kappa = 0,05$  is taken both for neutrons and for protons (the notation for  $\kappa$  and  $\mu$  agrees with the one of the Nilsson paper<sup>12/</sup>). Thus, all the level scheme is the same as in the variant 2 of ref.<sup>3/</sup>. It should correspond to the scheme that is in the best agreement with the empirical data on the level spectra of odd-A nuclei<sup>4/</sup>.

The values of the pairing force strength  $G$  are used also the same as in ref.<sup>/3/</sup>, i.e.  $G_n = (26,04/A)$  MeV for neutrons and  $G_p = (32,20/A)$  MeV for protons, with the 24 levels nearest to the Fermi surface taken into account for the pairing interaction.

The eqs. (4) are solved for  $84 \leq Z \leq 104$  and  $128 \leq N \leq 158$  for seven values of the deformation  $\eta = 0,2,3,4,5,6,7$ . The single-particle energies (and also the matrix elements  $q_{\nu\nu}$  for the calculation of  $Q_0$ ) for  $\eta = 3$  and 5 and for  $\eta = 7$  (for which the single-particle energies and wave functions are not given in refs.<sup>/12,4/</sup>) are obtained from the corresponding values for  $\eta = 2,4,6$ , by a quadratic interpolation and extrapolation, respectively.

The ground state energy is calculated from eq. (7) for  $\eta = 0,2,3,4,5,6,7$  and the corresponding curves are drawn in two variants: including the Coulomb term  $\epsilon_c$  (as in eq. (7)) and not including. In both cases the points of minimal energy (i.e. the equilibrium deformations  $\eta_{e,q}$  or  $\epsilon_{e,q}$  with  $\eta$  and  $\epsilon$  defined in ref.<sup>/12/</sup>) are obtained by a graphical interpolation.

In the present investigation the electrostatic energy of a sphere  $\epsilon_c(0)$  (and the integral in eq. (10)) is calculated assuming the radial charge distribution in the form of a step function with the radius of the sphere  $R_0 = 1,2 A^{1/3}$  fm, instead of the trapezoidal form adopted in ref.<sup>/3/</sup>. The effect of using one or the other form of the distribution on the equilibrium deformation is small<sup>/2/</sup>.

The electric quadrupole moment  $Q_0$  is calculated from eq. (6) for  $\eta = 0,2,3,4,5,6,7$ , and the values corresponding to the equilibrium deformation are obtained by a graphical interpolation.

All the numerical values of the ground state energy and quadrupole moment as well as the values of  $\lambda$  and  $\Delta^2$  (for these see also ref.<sup>/13/</sup>) calculated for  $\eta = 0,2,3,4,5,6,7$ ,  $Z = 84 - 104$  and  $N = 128 - 158$  are gathered in separate tables<sup>/14/</sup>. The results obtained with the BCS wave functions and in the case of no pairing forces are also given there, for comparison.

It should be stressed that in all the calculations the levels from the  $N=7$  shell for protons and from the  $N=8$  shell for neutrons have not been taken into account. We do not simply know their positions. Some extrapolations for the lowest levels of these shells, performed with the help of the Nilsson potential on one hand and with the Woods-Saxon potential, on the other, give different results (in the sense of the level sequence)<sup>/15/</sup>. One may expect, basing on these extrapolations, that the inclusion of these levels should not change the results for the equilibrium deformations, quadrupole moments and deformation energies for  $Z < 100$

and  $N < 148$  and that it might increase these quantities for the larger values of  $Z$  and  $N$ .

### 3. Results and Discussion

Fig. 1. gives an example of the dependence of the ground state energy on the deformation, for  $^{244}\text{Cm}$ . The independent particle curve (IP) is obtained by summing the Nilsson energies from the lowest one up to the Fermi energy, i.e. it is obtained in the same way as in refs.<sup>[4,5]</sup>. The BCS and PBCS curves are calculated with the help of the BCS and PBCS wave functions, respectively. The PBCS curve is drawn for two cases, when the Coulomb term  $\delta_C$  in eq. (7) is included (C) and not (NC).

It is seen that although the PBCS energy is lower for a few MeV than the BCS one, the dependences of the both energies on the deformation do not differ much. Thus the equilibrium deformations in both cases are almost the same and the deformation energies are close one to the other. Namely, the BCS deformation energy is about 1 MeV lower than the PBCS one, what represents about 14% of the PBCS value of the deformation energy in the NC case and about 9% in the C case.

Fig. 1(b) presents, for comparison, the potential energy curve (MS) of the liquid drop model supplemented by the deformation dependent shell correction<sup>[16,7]</sup> (for the shell correction see also ref.<sup>[17]</sup>). The values of the seven parameters of the semi-empirical model<sup>[16]</sup> are taken from the analysis by Myers and Swiatecki<sup>[7]</sup> in which the parameters are fitted to experimental nuclear masses and quadrupole moments.

Table 2 gives the equilibrium deformations  $\epsilon_{eq}$  calculated with the PBCS wave functions both with the Coulomb term included and not included. The equilibrium deformations obtained in ref.<sup>[3]</sup> (variant 2 corresponding to the same single-particle energy scheme as in the present paper) with the BCS functions and the deformations obtained in ref.<sup>[5]</sup> in the independent particle approximation (IP) are also given for comparison. The last values are read from the diagram of ref.<sup>[5]</sup>. The additional single-particle level shifts used in ref.<sup>[5]</sup> are close to the ones of our paper. The slight differences are such that they may result in making the nuclei at the beginning of the investigated region slightly softer on the deformation in the case of our additional shifts. It can be possibly seen in table 2 (see  $^{244}\text{Ra}$ ).

We see in Fig.1 for  $^{244}\text{Cm}$  that the inclusion of the pairing interaction together with the Coulomb term to the ground state energy increases  $\epsilon_{eq}$ , i.e.



that in the competition to change the equilibrium deformation in the opposite directions, the Coulomb term predominates over the pairing forces. Table 2 shows that this effect is typical for almost the whole region, excluding only the most weakly deformed nuclei at the beginning of the region. Moreover, the values of  $\epsilon_{eq}$  obtained in the independent particle case are closer to the PBCS ones calculated without Coulomb term (NC) than to these with Coulomb term (C). The effect was also observed in the rare earth region, especially for the most strongly deformed nuclei<sup>[1]</sup>.

Fig. 2. gives the ground state electric quadrupole moments. The experimental points obtained from measurements of the lifetimes of the first excited  $2+$  states are cited here after ref.<sup>[18]</sup>. The points corresponding to Coulomb excitation data are deduced from the  $B(E2)$  values collected in ref.<sup>[19]</sup>. The comparison between the PBCS and the BCS results (including the Coulomb term) shows that they are close one to the other. The PBCS calculation predicts the deformation to appear slightly earlier (see  $^{222}\text{Ra}$ ,  $^{224}\text{Th}$ ) and gives the  $Q_0$  values closer to experiment at the beginning of the region. The remaining discrepancy between the theory and experiment for these nuclei may be partly due to the fact that the experimental  $Q_0$  values are obtained from the measurement under the assumption of the adiabaticity condition, which in this transition region is not fulfilled well.

Fig. 3 shows the dependence of the quadrupole moment  $Q_0$ , calculated with the PBCS wave function, on the deformation for  $Z = 96$ . The BCS values of  $Q_0$  are quite close to the PBCS ones, so that the corresponding curve would not be distinguishable from the curve plotted in Fig. 3.

Fig. 4 presents the deformation energies. Two of the five presented curves are obtained with the PBCS wave functions, including the Coulomb term (C) and not including (NC). The independent particle curve (IP) is read from the diagram of ref.<sup>[5]</sup>. The last two curves are deduced from the analysis by Myers and Swiatecki<sup>[7]</sup> (see also another semi-empirical analysis<sup>[20]</sup> allowing larger number of adjustable parameters. It predicts smaller values of the deformation energy). The curve denoted "semi-emp MS" is obtained from the calculated one ("calc MS") by taking the experimental mass of a nucleus instead of the mass calculated for the equilibrium point.

One can see that the PBCS results obtained without the Coulomb term (NC) are the closest ones to the semi-empirical estimates, although in comparison with the situation in the rare region, a tendency of the decrease of the discrepancy between the semi-empirical estimates and the C variant of the theoretical results is visible. However, comparing the calculated values with the semi-empirical ones (especially for the heaviest nuclei), it should be remembered that the last ones

have been obtained under the assumption of the magic numbers  $N = 184$  and  $Z = 126$ , closing the deformation region of the heavy elements. The level scheme used in the present calculation does not reproduce these numbers well<sup>15/</sup>.

Table 3 gives the values of the density deformation parameter  $\bar{\epsilon}$  obtained with the help of eq. (10) from the quadrupole moments  $Q_0$  calculated from the formulae (6) and (8) for the deformations of the potential  $\epsilon = 0,10, 0,20$  and  $0,30$ . It is seen that for  $Z = 88 - 104$  the difference between  $\epsilon$  and  $\bar{\epsilon}$  does not exceed 10 %.

As mentioned in the introduction, it is interesting to check explicitly what part of the Coulomb repulsion is already taken into account by the use of the single-particle energy levels for protons different than these for neutrons. With this aim, the calculation of the ground state energy for  $N$  neutrons with the help of the neutron single-particle level scheme and of the ground state energy for  $Z$  protons with the help of the proton scheme is performed. The dependence of the difference  $\Delta \bar{\epsilon}_{pn} \equiv \bar{\epsilon}_p(\eta) - \bar{\epsilon}_n(\eta) - [\bar{\epsilon}_p(0) - \bar{\epsilon}_n(0)]$  on the deformation for  $N = Z = 96, 98, 104$  is plotted in Fig. 5. The decrease  $\Delta \bar{\epsilon}_C \equiv \bar{\epsilon}_C(\eta) - \bar{\epsilon}_C(0)$  of the electrostatic Coulomb term  $\bar{\epsilon}_C$  calculated from the formula (9) is drawn for comparison.

The form of the curves suggests that the  $\Delta \bar{\epsilon}_{pn}$  term has stronger effect on the deformation energy than on the equilibrium deformation. For example, the effect of this term on the equilibrium deformations of the three nuclei:  $^{244}\text{Cm}$ ,  $^{248}\text{Cf}$  and  $^{268}\text{Cf}$  (104) is  $\Delta \epsilon \leq 0,01$  (while the effect of the  $\Delta \bar{\epsilon}_C$  term is  $\Delta \epsilon = 0,03$ ), what corresponds to the change in the quadrupole moments  $\Delta Q_0 \leq 0,4$  barn. The corresponding effect on the deformation energy is 2,0 MeV for  $^{244}\text{Cm}$  and  $^{248}\text{Cf}$ , 1,1 MeV for  $^{268}\text{Cf}$  (104), so that the subtraction of the  $\Delta \bar{\epsilon}_{pn}$  term from the ground state energy decreases the discrepancy between the C variant of the calculation and the semi-empirical estimate by about 50% for these three nuclei.

If the effect of the  $\Delta \bar{\epsilon}_{pn}$  term on the equilibrium deformations and hence on the quadrupole moments of the other nuclei in the heavy element region and also in the rare earth region is as small as for the three nuclei considered, one should look for other reasons for the obtained discrepancies between the calculated quadrupole moments and the experimental ones. A possible one is a too high increase of the restoring force of the closed shells in the volume-preserving harmonic oscillator potential (and also in the Nilsson potential) with the increasing mass number  $A$ . As the energy of a nucleus with closed shells in this model is

$$\sum_{\nu} 2\epsilon_{\nu} \propto \hbar \omega_0(\epsilon) A^{4/3} \propto \left[ 1 - \frac{1}{3} \epsilon^2 - \frac{2}{27} \epsilon^3 \right]^{-1/3} A,$$

the restoring force is proportional to  $A$ . In the liquid drop-plus-shell correction model<sup>[16,7]</sup>, which reproduces the boundary points of the deformation regions and even the values of the quadrupole moments quite well, the restoring force is proportional to something between  $A^{2/3}$  (surface term) and  $A$  (shell correction). An explicit comparison of the dependences of the BCS and PBCS ground state energies and of the potential energy in the semi-empirical model<sup>[7]</sup>, on the deformation, is given in Fig. 6 for  $^{142}\text{Ce}$ ,  $^{190}\text{Pt}$ , and  $^{212}\text{Po}$ . It is seen that the BCS and PBCS calculations predict the restoring force for  $^{142}\text{Ce}$  much lower than the one predicted by the semi-empirical model. Only after the reduction of the semi-empirical restoring force by the Coulomb term  $\Delta\tilde{\epsilon}_C$ , all the three curves become close one to each other. It is probably the reason why the  $Q_0$  results of the NC variant of the PBCS calculation are closer to experiment at the beginning of the rare earth region, than the results of the C variant.

For  $^{190}\text{Pt}$  (this nucleus is not the best example, as it is far enough from the double magic nucleus, to be deformed) and  $^{212}\text{Po}$  we obtain the opposite situation: the BCS and PBCS restoring forces are larger than the semi-empirical restoring force and possibly for this reason even the C variant of the PBCS calculations gives too low  $Q_0$  values in the second half of the rare earth region and in the whole heavy element region.

#### 4. Conclusions

The calculations of the equilibrium deformations, electric quadrupole moments and deformation energies, performed both for the rare earth region and the heavy element one, lead to following conclusions:

##### 4.1. Equilibrium Deformations and Quadrupole Moments

(a) It seems that the equilibrium deformations and the quadrupole moments should be described by the variant of the calculation which includes the Coulomb term  $\tilde{\epsilon}_C$  (variant C), but in which the  $\Delta\tilde{\epsilon}_{pn}$  term is subtracted from the energy. The considered examples of nuclei ( $^{244}\text{Cm}$ ,  $^{248}\text{Cf}$  and  $^{288}(104)$ ) suggest that the subtraction of the  $\Delta\tilde{\epsilon}_{pn}$  term has only slight (in comparison with the subtraction of the  $\Delta\tilde{\epsilon}_C$  term) effect on the equilibrium deformation and thus on the quadrupole moment. The fact that the NC variant gives better results for the beginning of the rare earth region up to Dy isotopes, is probably due to the too low restoring force implied for these nuclei by the volume-preserving model we use. Dropping the Coulomb term we only increase this too low restoring force.

For the nuclei heavier than Dy isotopes, both in the rare earth region and in the heavy element one, the quadrupole moments are better reproduced by the C variant of the calculation and even this variant gives the results lower than experiment for almost all the nuclei.

(b) The effect of the pairing forces on the equilibrium deformation is small, except for nuclei at the boundaries of the deformation regions.

It does not compensate the effect of the Coulomb term  $\delta_c$ , so that the equilibrium deformations obtained taking both the pairing and the Coulomb interactions into account are, excluding nuclei at the boundaries of the regions, larger than the ones calculated in the independent particle approximation.

(c) The use of the PBCS wave functions instead of the BCS ones results, in the rare earth region, in a decrease of the restoring force (and thus in an increase of the equilibrium deformation): slight in the middle of the region and stronger at its boundaries. Thus, it improves the results only for the nuclei for which the restoring force obtained with the BCS wave functions is too large, i.e. for the nuclei in the second half of the region. For the heavy elements an improvement of the results is obtained for nuclei at the beginning of the region.

#### 4.2. Deformation Energies

(a) Pairing forces decrease the deformation energy significantly and make it closer to the values obtained from the semi-empirical estimates<sup>[7]</sup> in the both regions of deformed nuclei.

(b) The comparison between the calculated deformation energies and the semi-empirical ones, similarly as the comparison between the calculated quadrupole moments and the experimental ones, suggests that the restoring force in the model we use is too low at the beginning of the rare earth region and it increases too quickly with the increasing mass number A.

(c) The effect of the  $\Delta\delta_{pn}$  term seems to be important for the deformation energies. After taking it into account for Cm and Cf isotopes, the discrepancy between the calculated results (variant C) and the semi-empirical estimates decreases by about 2 MeV.

The author wishes to express his gratitude to V.G. Soloviev and Z. Szyman-ski for suggesting the problem and valuable remarks. He would also like to thank Z. Bochnacki, I.M. Mikhailov, V.V. Pashkevich and P. Vogel for helpful discussions.

The use of the matrix elements  $q_{\nu\nu}$  calculated by G. Jungclaussen and A.A. Korneichuk is gratefully acknowledged. In conclusion it is a pleasure for

the author to thank I.N. Kukhtina for performing the numerical calculations on an electronic computer.

### References

1. A. Sobiczewski. Nuclear Physics, (in print.)
2. D.R. Bes and Z. Szymanski. Nuclear Physics, 28 (1961) 42
3. Z. Szymanski. Nuclear Physics, 28 (1961) 63; Acta Phys. Polon., 23 (1963) 543
4. B.R. Mottelson and S.G. Nilsson. Mat. Fys. Skr. Dan. Vid. Selsk., 1, No.8 (1959)
5. E. Marshalek, L.W. Person and R.K. Sheline. Revs. Mod. Phys., 35 (1963) 108
6. R.A. Demirkhanov, V.V. Dorokhov, V.G. Soloviev. Yadernaya Fizika (USSR), 2, (1965) 10
7. W.L. Myers and W.J. Swiatecki. Report UCRL- 11980 (1965)
8. H.J. Mang, J.K. Poggenburg and J.O. Rasmussen. Nuclear Physics, 64 (1965) 353
9. J. Bardeen, L.N. Cooper and J.R. Schrieffer. Phys. Rev., 108 (1957) 1175
10. M.K. Volkov, A. Pawlikowski, W. Rybarska and V.G. Soloviev. Izv. Akad. Nauk SSSR, 27 (1963) 878
11. B.C. Carlson. J. Math. Phys., 2, 441 (1961).
12. S.G. Nilsson. Mat. Fys. Medd. Dan. Vid. Selsk., 29, N.16 (1955)
13. Z. Szymanski. Report No. 230/VII, Institute for Nuclear Research Warsaw, 1961
14. I.N. Kukhtina and A. Sobiczewski. Preprint E-4-2940, Dubna, 1966.
15. A. Sobiczewski, F.A. Gareev, and B.N. Kalinkin. Phys. Lett., 22, 500 (1966).
16. W.J. Swiatecki, in Proc. Second Int. Conf. on Nuclidic Masses, Vienna, Austria, July 15 - 19, 1963, ed by W.H. Johnson, Jr. (Springer-Verlag, Vienna, 1964) p. 58
17. V.M. Strutinsky. Yadernaya Fizika (USSR), 3 (1966) 614
18. S. Björnholm. Radiochemical and Spectroscopic Studies of Nuclear Excitations in Even Isotopes of the Heaviest Elements (Munksgaard, Copenhagen, 1965)
19. J. Lindskog, T. Sundström and R. Sparrman. In Perturbed angular correlations, ed by E. Karrlsson, E. Mathias and K. Siegbahn (North-Holland Publ. Co., Amsterdam, 1964) appendix 2
20. H. Kummel, J.H.E. Mattauch, W. Thiele and A.H. Wapstra. Nuclear Physics, 81 (1966) 129

Received by Publishing Department  
on September 19, 1966

Table 1. Values of the parameters and the additional shifts of the single-particle energy levels used in the calculations.

Shells		$\mu$	Additional shifts [in $\hbar\omega_0$ ]	
Neutrons $N > 126$	$N = 5$	0.45	-0.23	all levels
	$N = 6$	0.45	-0.08	$i \frac{13}{2}$
	$N = 7$	0.40	-0.06	$j \frac{15}{2}$
Protons $Z > 82$	$N = 4$	0.55	-0.23	all levels
	$N = 5$	0.70	-0.05	$h \frac{11}{2}$
	$N = 6$	0.45	-0.35	$i \frac{13}{2}$

Table 3. The values of the density deformation parameter  $\bar{\epsilon}$  as a function of the potential deformation  $\epsilon$ .

Z	$\bar{\epsilon}$		
	$\epsilon = 0.10$	$\epsilon = 0.20$	$\epsilon = 0.30$
84	0.07	0.17	0.30
86	0.08	0.17	0.30
88	0.09	0.18	0.29
90	0.09	0.18	0.29
92	0.10	0.19	0.29
94	0.10	0.20	0.28
96	0.11	0.20	0.28
98	0.11	0.20	0.27
100	0.11	0.20	0.27
102	0.11	0.20	0.27
104	0.11	0.20	0.27

Table 2. Equilibrium deformations  $\epsilon_{eq}$ . The second and the third columns give the values for the PBCS case with the Coulomb term included, and not included, respectively. The results of ref. [3] and of ref. [5] are quoted in the fourth and in the fifth columns, respectively.

Nucleus	PBCS		IP	Nucleus	PBCS		IP		
	C	NC			C	NC			
222 <sub>Em</sub>	0	0	0	0.08	238 <sub>Cm</sub>	0.23	0.20	0.24	0.20
224 <sub>Em</sub>	0.14	0	0.06	0.11	240 <sub>Cm</sub>	0.23	0.21	0.24	0.21
220 <sub>Ra</sub>	0	0	0		242 <sub>Cm</sub>	0.24	0.21	0.24	0.21
222 <sub>Ra</sub>	0.10	0	0	0.08	244 <sub>Cm</sub>	0.24	0.22	0.24	0.22
224 <sub>Ra</sub>	0.13	0.11	0.08	0.08	246 <sub>Cm</sub>	0.24	0.22	0.24	0.22
226 <sub>Ra</sub>	0.15	0.13	0.12	0.13	248 <sub>Cm</sub>	0.24	0.21	0.24	0.22
228 <sub>Ra</sub>	0.17	0.14	0.16	0.15	250 <sub>Cm</sub>	0.24	0.20		0.21
230 <sub>Ra</sub>	0.19	0.15	0.21	0.17	244 <sub>Cf</sub>	0.24	0.21	0.24	0.21
224 <sub>Th</sub>	0.13	0	0	0.11	246 <sub>Cf</sub>	0.24	0.22	0.24	0.22
226 <sub>Th</sub>	0.15	0.12	0.12	0.13	248 <sub>Cf</sub>	0.24	0.22	0.24	0.22
228 <sub>Th</sub>	0.17	0.14	0.16	0.17	250 <sub>Cf</sub>	0.24	0.21	0.24	0.22
230 <sub>Th</sub>	0.19	0.15	0.20	0.17	252 <sub>Cf</sub>	0.24	0.20		0.21
232 <sub>Th</sub>	0.21	0.17	0.23	0.17	254 <sub>Cf</sub>	0.23	0.19		0.20
234 <sub>Th</sub>	0.23	0.18	0.24	0.19	248 <sub>Fm</sub>	0.24	0.22	0.24	0.22
228 <sub>U</sub>	0.18	0.14	0.15	0.15	250 <sub>Fm</sub>	0.24	0.22	0.24	0.22
230 <sub>U</sub>	0.20	0.16	0.21	0.17	252 <sub>Fm</sub>	0.24	0.21	0.24	0.22
232 <sub>U</sub>	0.21	0.17	0.24	0.18	254 <sub>Fm</sub>	0.24	0.20		0.21
234 <sub>U</sub>	0.22	0.18	0.25	0.19	256 <sub>Fm</sub>	0.23	0.19		0.20
236 <sub>U</sub>	0.22	0.19	0.24	0.19	258 <sub>Fm</sub>	0.23	0.19		0.20
238 <sub>U</sub>	0.23	0.20	0.24	0.20	252(102)	0.23	0.21		0.21
240 <sub>U</sub>	0.24	0.20	0.24	0.21	254(102)	0.23	0.21		0.21
232 <sub>Pu</sub>	0.22	0.17	0.24	0.17	256(102)	0.22	0.20		0.21
234 <sub>Pu</sub>	0.23	0.18	0.24	0.19	258(102)	0.22	0.19		0.20
236 <sub>Pu</sub>	0.23	0.19	0.24	0.19	260(102)	0.22	0.19		0.20
238 <sub>Pu</sub>	0.23	0.20	0.24	0.20	254(104)	0.23	0.20		0.21
240 <sub>Pu</sub>	0.23	0.20	0.24	0.20	256(104)	0.23	0.20		0.21
242 <sub>Pu</sub>	0.24	0.21	0.24	0.21	258(104)	0.22	0.19		0.19
244 <sub>Pu</sub>	0.24	0.21	0.24	0.21	260(104)	0.22	0.19		0.19
246 <sub>Pu</sub>	0.24	0.21	0.24	0.21	262(104)	0.21	0.18		0.19

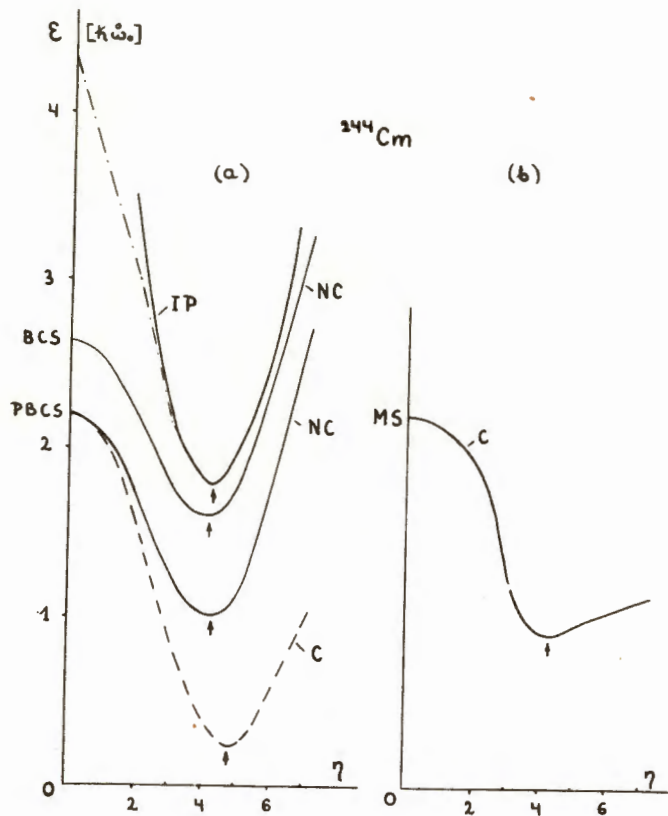


Fig. 1. The dependence of the ground state energy (in  $h\omega_0 = 41 A^{-1/3}$  MeV) on the deformation for  $^{244}\text{Cm}$ .  
 (a) The energy calculated using three types of the wave functions: independent particle (IP), BCS and PBCS. The IP solid line corresponds to the configuration giving the absolute minimum. The IP dotted-dashed line connects the ground state energy points for  $\eta = 0, 2, 3, 4$ . The solid lines for the BCS and PBCS cases correspond to the energy with no Coulomb term (NC). The dashed line for the PBCS case corresponds to the energy with the decrease (i.e.  $\delta_c(\eta) - \delta_c(0)$ ) of the Coulomb term included (C).  
 (b) The dependence of the energy on the deformation, obtained from the Myers and Swiatecki semi-empirical analysis.

The arrows indicate the minimum points. The zero point of the energy is taken arbitrarily.

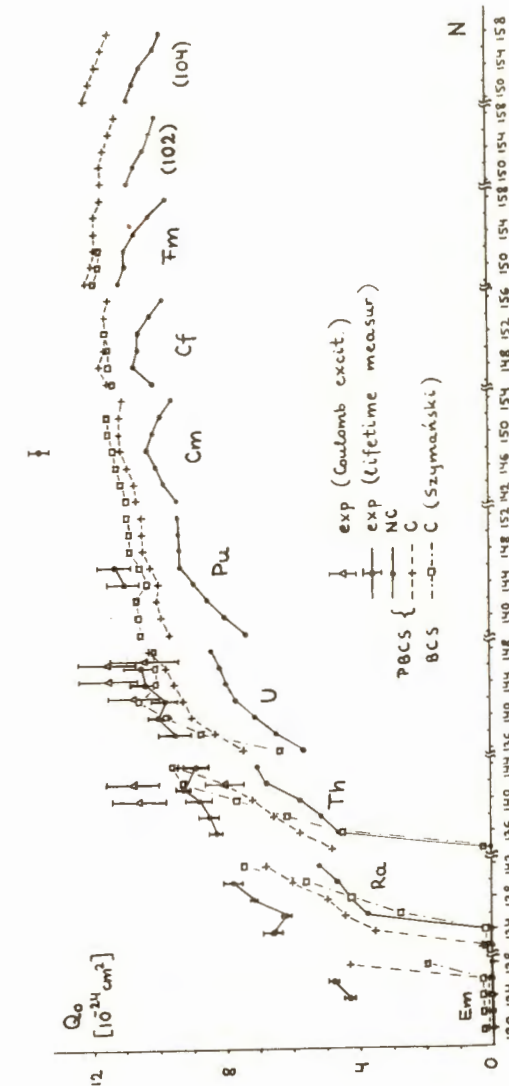


Fig. 2. Equilibrium quadrupole moments  $Q_0$  versus neutron number  $N$ .

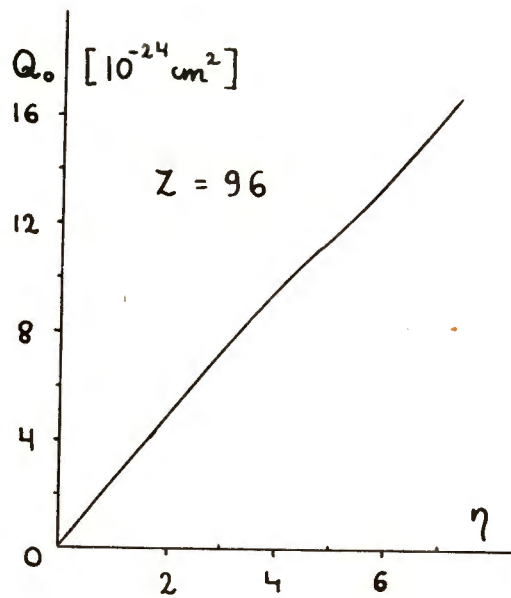


Fig. 3. The dependence of the quadrupole moment on the deformation for  $Z = 96$ .

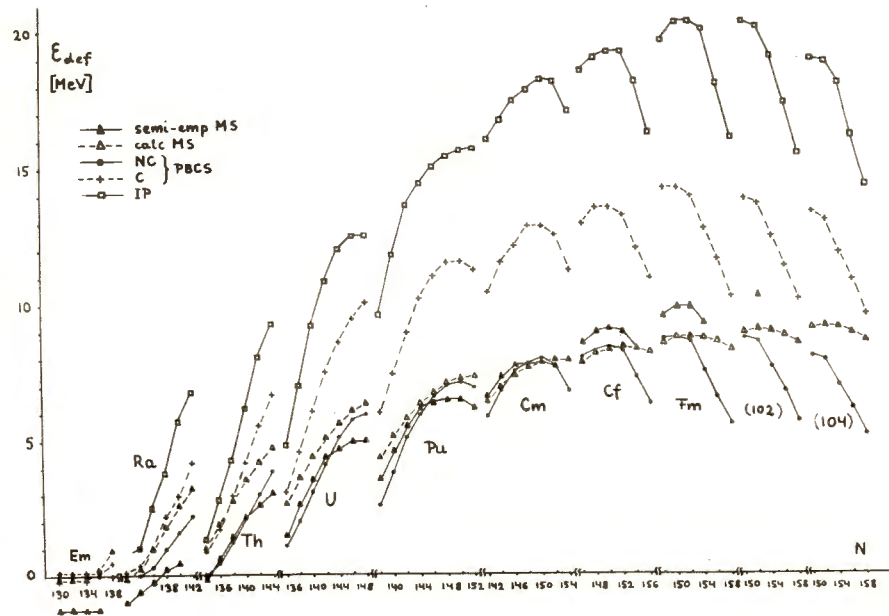


Fig. 4. Deformation energy in MeV versus neutron number  $N$ . Open and closed triangles correspond to the deformation energy deduced from the Myers and Swiatecki semi-empirical analysis.



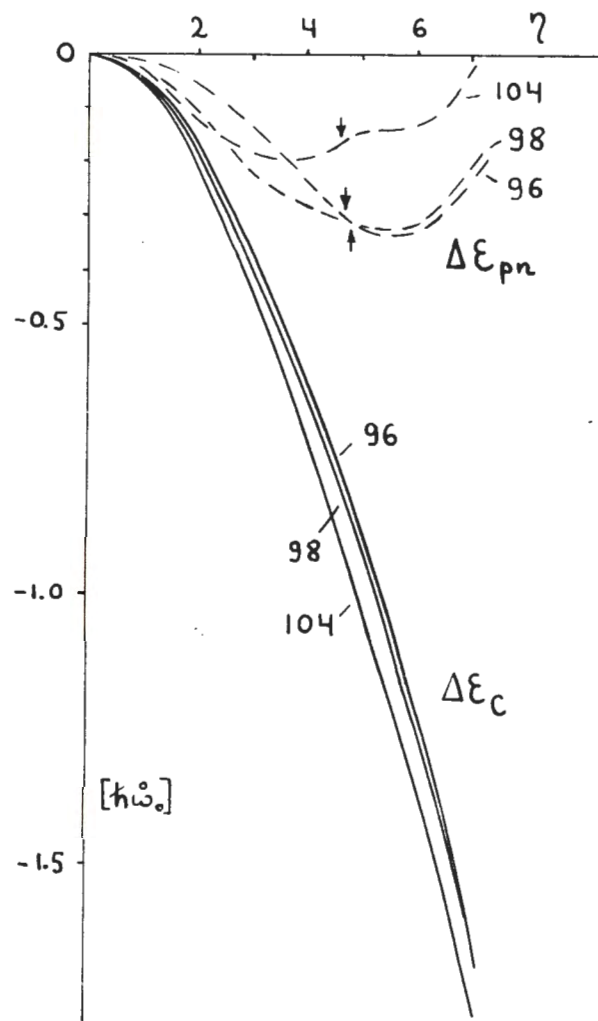


Fig. 5. The difference  $\Delta\epsilon_{pn}$  of the ground state energies of protons and N neutrons as a function of the deformation.  $N = Z = 96, 98, 104$ . The dependence of the electrostatic Coulomb term  $\Delta\epsilon_C$  on the deformation is plotted for comparison. The arrows indicate the equilibrium points for the nuclei:  $^{244}\text{Cm}$ ,  $^{248}\text{Cf}$  and  $^{288}(104)$ .

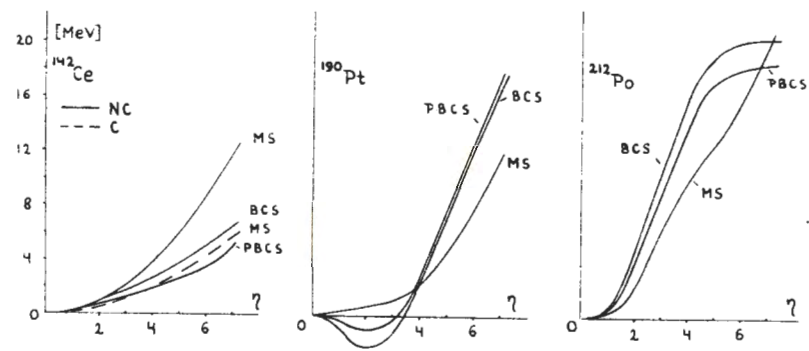


Fig. 6. The ground state energy curves obtained in the BCS and PBCS calculations and the potential energy curves calculated in the liquid drop-plus-shell correction model